Accepted Manuscript

Effect of high strain rate on glass/carbon/hybrid fiber reinforced epoxy laminated composites

K. Naresh, K. Shankar, B.S. Rao, R. Velmurugan

PII: S1359-8368(16)30901-5

DOI: 10.1016/j.compositesb.2016.06.007

Reference: JCOMB 4352

To appear in: *Composites Part B*

Received Date: 30 January 2016

Revised Date: 25 May 2016

Accepted Date: 3 June 2016

Please cite this article as: Naresh K, Shankar K, Rao BS, Velmurugan R, Effect of high strain rate on glass/carbon/hybrid fiber reinforced epoxy laminated composites, *Composites Part B* (2016), doi: 10.1016/j.compositesb.2016.06.007.

EFFECT OF HIGH STRAIN RATE ON GLASS/CARBON/HYBRID FIBER REINFORCED EPOXY LAMINATED COMPOSITES

K. Naresh[1], K. Shankar[1], B.S. Rao[2] and R.Velmurugan[3*]

[1]*Department of Mechanical Engineering, Indian Institute of Technology Madras, Chennai, India*
[2]*Aeronautical Development Agency, Bangalore, India*
[3]*Department of Aerospace Engineering, Indian Institute of Technology Madras, Chennai, India*

[*]Corresponding author: ramanv@iitm.ac.in, +91 44 22574017

Abstract

Composites are efficient, to deal with tensile loads, than metals. Now-a-days, metals are replaced with composites owing to their higher strength to weight ratio and are extensively used in aircraft wing and fuselage structures. These structures are subjected to high strain rates during impact loadings, such as bird hit or run-way debris impact. In order to design robust composite structures, it is important to understand the strain-rate-dependent behavior of composite materials. In this study, influence of strain rate on the tensile properties of glass/epoxy, carbon/epoxy and hybrid (glass-carbon/epoxy) composites are experimentally and theoretically investigated in the range of strain rates from 0.0016 s^{-1} to 542 s^{-1}. Drop mass setup is used for high strain rate tests. Quasi-static tests are performed on Instron universal testing machine in accordance with ASTM D638. The results indicate that the tensile strength and tensile modulus of GFRP and hybrid composites increase and percentage of failure strain for GFRP, CFRP and Hybrid composites decreases with the increase in strain rate, whereas tensile strength and tensile modulus of CFRP remains approximately constant. The scanning electron microscopy is used for analyzing the failure modes of the failed region (surface) of the tested specimens. Non contact DIC system is used to capture the strain field with the help of high speed camera.

1. Introduction

Now-a-days, the use of composite materials is increasing very rapidly and particularly their use in aerospace, defense and automotive applications are inevitable, because of their superior structural properties. At the same time, many accidents occurred because of

structural failures of components due to a bird hit on the aircraft, runway debris hit on gas turbine blades and many accidents in road and rail vehicles. Therefore a complete characterization of composite materials is very much required for the reliable design of structural components. Some of the experimental techniques are helpful to characterize the rate dependent behavior of the composite materials. The experimental techniques for dynamic loading are mainly categorized based on the final parameters to be tested which include, tensile, compression and shear loading and the range of strain rate experienced during testing**. Koerber et al**. **[1]** presented experimental study of the strain rate effect on unidirectional carbon/epoxy composites for strain rates up to 350 s^{-1} using SHPB. The in-plane strain field of the specimen was obtained by the digital image correlation technique by using a high speed camera. **Brown et al. [2]** studied the tensile, compression and shear behavior of commingled, woven E-glass/polypropylene composites for the strain rate range of 10^{-3} s^{-1} to 10^{2} s^{-1} using the universal testing machine and falling weight drop tower. It was observed that there was an increase in the compressive and tensile modulus and strength with increase of strain rate. However, the shear modulus and shear strength decreased with increasing strain rate. **Okoli et al. [3]** worked on high strain rate characterization of glass/epoxy composites under tensile and shear loading. It was reported that there was an increase in the mechanical properties such as tensile strength, shear strength, tensile modulus and shear modulus for the increase of strain rate. **Duan et al. [4]** investigated the mechanical properties of continuous, Glass Fiber Reinforced Polypropylene composites for the strain rates of 0.001 s^{-1} to 50 s^{-1}**.** They observed that ultimate strength and failure strain increase with the increase of strain rate. **Ochala et al. [5]** compared the dynamic compression response of GFRP and CFRP composites for the strain rates of 10^{-3} s^{-1} and 450 s^{-1} by using servo hydraulic machine and SHPB, respectively. It was observed that the compressive strength for GFRP increased with increasing strain rates and not much change of CFRP. The failure strain for both GFRP and CFRP decreased with increase in strain rates. **Gilat et al. [6]** investigated the strain rate effect on the tensile properties of carbon/epoxy material by using modified SHPB. The identical specimens with different orientation (90°,10°, 45°, $[\pm 45^{\circ}]_s$) were tested at strain rates of 10^{-5}, 1 and 400-600 s^{-1}. It was observed that in all the configurations stiffness increased with increasing strain rate. **Elanchezhian et al. [7]** studied the mechanical behavior of CFRP and GFRP composites for different temperatures and strain rates. They observed that the CFRP composites have better tensile and flexural properties compared to GFRP composites. **Guedes et al. [8]** have used unidirectional laminates for uniaxial compression tests on a universal testing machine at the strain rates of 0.07, 0.001 and 0.0001 s^{-1} and developed a 3-

parameter constitutive viscoplastic model to describe the mechanical behavior. Experimental studies on the strain rate effect of glass/epoxy/clay nanocomposites, in the strain rate ranges from 0.0016 to 450 s^{-1} were studied [**9]**. It is found that the glass/epoxy composite is strain rate sensitive and reveals that the tensile modulus and strength increase as the clay loading increases. **Alemi-Ardakani et al. [10]** have conducted experiments on twill woven glass/polypropylene composite laminates under the impact energy of 200 J using the drop weight machine and Abaqus/Explicit was used for modeling the laminate through Hashin progressive damage criterion and showed reasonably accurate results. **Rotem and Lifshitz [11]** studied the effect of strain rate ranges from 10^{-6} to 30 s^{-1} on the tensile behavior of unidirectional glass/epoxy composites. They found that the dynamic strength and modulus increased by 3 times and 50%, respectively, with respect to the static strength and modulus. Our studies **[12-13]** show that with the addition of clay the tensile modulus and strength increase even at low strain rates as strain rate increases for both epoxy and glass/epoxy nanocomposites. **Naik et al. [14]** described hybrid composites (glass-carbon/epoxy) reduced notch sensitivity and improved impact resistance. **Zweben [15-16]** has used hybrid ("Kevlar" 49 aramid – "thornel" 300 graphite/epoxy) composites for his study and found that the tensile failure strain and fracture toughness have increased for the hybrid effect. Hybrid composites are mainly used to obtain the combined advantages of two or more types of fibers or matrices or both and at the same time mitigating their less desirable properties **[17].** There are only few studies on the strain rate effect of hybrid (glass-carbon/epoxy) composites. Carbon/epoxy composite is stiffer material and less sensitive to strain rate, but glass/epoxy composite is more sensitive to strain rate. The combination of these two fibers will make a laminate which is sensitive and stiffer to impact loading. Hence, in the present study in addition to glass/epoxy and carbon/epoxy composite we have used hybrid (glass-carbon/epoxy) composite material to characterize the tensile behavior for different strain rates.

The present research work is to investigate the influence of strain rate, in the range of 0.0016 s^{-1} to 542 s^{-1}, on the tensile strength, tensile modulus, and failure strain of glass/epoxy, carbon/epoxy and hybrid composites. The results obtained in this investigation show that the percentage of failure strain for GFRP, CFRP and hybrid composites decreases and the tensile strength and tensile modulus of GFRP and hybrid composites increase with the increase in strain rate, whereas tensile strength and tensile modulus of CFRP remains approximately constant. Theoretical studies show good correlation with experiments. The DIC system is useful to get the strain field at different levels of deformation.

2. Experimental setup

2.1. Drop mass setup

Drop weight impact machine is used for dynamic testing to produce strain rates from 10 to 1000 s^{-1} **[18-19]**. In this technique the weight is dropped from a pre-determined height to strike the test specimen located in the fixture. Height of falling weight along with the specimen geometry is responsible for achieving different strain rates. Load cells and non-contact strain measuring methods are used for calculating stress and strain respectively. The drop mass setup mainly consists of a base plate, a drop mass tower, an elevator, a magnetic holder and a fixture for holding specimen as shown in Fig. 1. The guide rods, which are made of hard chrome plated steel, are used to guide the falling mass. The falling mass is set at heights of 0.25, 0.5, 0.75, 1, 1.25 and 1.5 m to attain velocities of 2.21, 3.13, 3.83, 4.43, 4.95 and 5.42 ms^{-1} respectively. These velocities are responsible for nominal strain rates of 221, 313, 384, 443, 495 and 542 s^{-1} on the specimen. The schematic diagram of the drop mass tower and the specimen fixture is shown in Fig. 1.

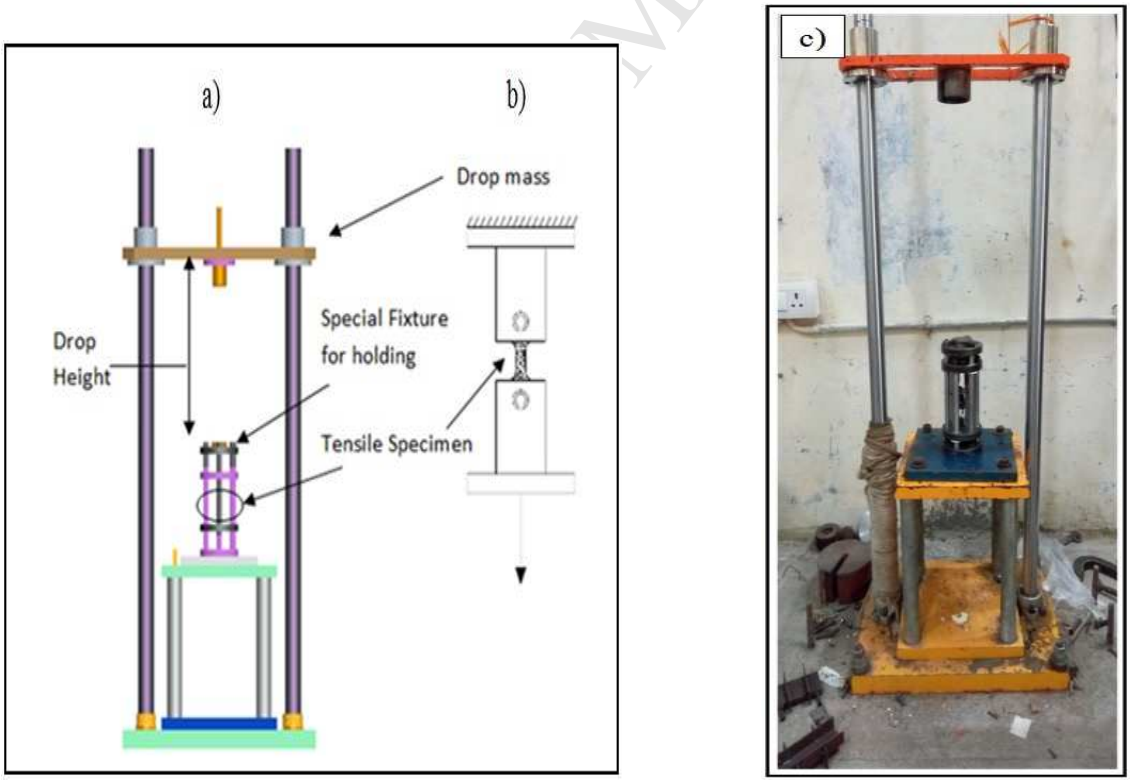

Fig. 1 Schematic diagram of drop tower a) Test setup model b) Specimen fixture c) Experimental setup

The piezoelectric load cell (PCB 208C04) of capacity 5 KN is used to measure the applied load. The stress data is calculated by dividing load data with the cross section area of gauge portion. A high speed camera (Phantom V611) with a maximum resolution of 1280x800 is used for capturing images. At full resolution, we can achieve a speed of 6246 frames per second and at lower resolutions it can deliver up to 1, 00,000 fps. Due to the smaller area of interest, a high frame-rate of 100,000 fps is achieved at a resolution of 128 x 128 pixels with exposure time of 9.81 µs. The data acquisition system, NI PXI 1042 along with the lab view, is used for acquiring the load data from the load cell. Light emitting diode (LED) panel lights of 30 W capacity is used as a lighting system. Proper lighting is required to ensure better quality pictures.

3. Material selection and laminate preparation

Three types of composite laminates, viz glass/epoxy, carbon/epoxy and hybrid (glass-carbon/epoxy) are considered for the study. The E-Glass fibre, woven roving mat, plain weave, 610 gsm, from Shakthi fibre glass, Chennai, India and carbon fibre of plane weave type, 450 gsm and woven roving mat from Hindustan mills Pvt Limited, Pune, India are used. Epoxy (Araldite (LY556)) and Hardener (HY951) are used as resin system. The mixing ratios by weight for fibre to resin and resin to hardener are maintained as 1:1 and 10:1, respectively. The laminates of 300x300 mm with thickness of 2 mm are made by compression moulding technique. All the laminates are made with a layup of [$0^{\circ}/90^{\circ}$] orientation. Each layer of the laminate has an average thickness of 0.4 mm. The spacer of 2 mm thickness is used for maintaining thickness of the laminate and the straight fibre direction is ensured by taking proper care.

4. Specimen preparation and geometry

There are no specific data available on geometry of the high strain rate specimen for laminated composites, however, based on literature survey and by trial and error, the new specimen geometry (Fig. 2) is designed and validated by using the drop weight dynamic test.

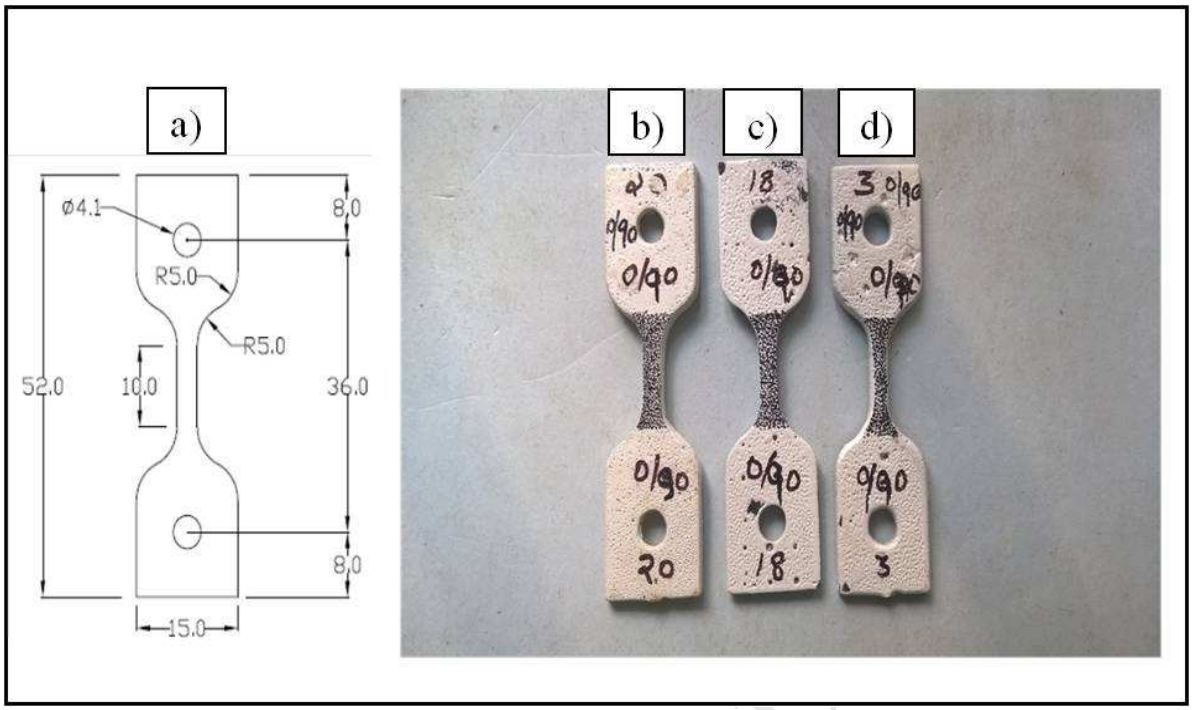

Fig. 2 High strain rate specimen geometry a) AutoCAD diagram b) GFRP composites specimen c) Hybrid (glass-carbon/epoxy) composites specimen d) CFRP composites specimen

It consists of a central zone with a constant width of 3 mm, gauge length of 10 mm and both ends with a hole of 4 mm diameter. Width from the central zone to ends increases gradually with a circular curve of radius 5 mm. The dimensions of reference geometry are established by trials and the dimensions are in accordance with ASTM D638.

4.1. Speckle pattern on specimen

The digital image correlation technique (DIC) is used to measure planar deformations and in-plane strains by the application of speckle pattern on the test specimen surface. The speckle pattern on the specimen can be achieved through different ways like spraying paints on the specimen by pressurized spray paint, by using tooth brushes and also by putting random dots on the specimen manually with special OHP markers.

5. Results and discussion

The mechanical properties of all specimens (glass/carbon/hybrid) are tested at strain rate ranges from 0.0016 s^{-1} to 542 s^{-1}. For quasi-static, 3 specimens for each laminate are tested at

a cross-head speed of 5 mm/min and the values are given in Table 1. In dynamic studies, 5 specimens for each laminate variant and for each strain rate, total of 30 specimens are tested and the mean value of the experimental results are given in Tables 2-4.

5.1. Stress analysis

The data acquisition was sourced from National instruments (NI PXI 1042). Stress values obtained from the load data (P) are obtained from a different strain rates. The stress-strain curves at strain rates of 0.0016, 221, 313, 384, 443, 495 and 542 s^{-1} are shown in Figs. 9-11. The nominal strain rates are calculated from the relation **[20]**

$$\dot{\varepsilon} = \frac{V}{L_0} \qquad (1)$$

in which L_o is the gauge length of the specimen, which is 10 mm for the dynamic specimens and V is the impact velocity. The impact velocity is obtained by the equation

$$V = \sqrt{2gh} \qquad (2)$$

Where

g is gravitational pull and h is height of falling weight.

The modulus value for cross ply laminates is obtained by the expression

$$E_x = E_y = \frac{1}{h}\frac{A_{11}^2 - A_{12}^2}{A_{11}} \qquad (3)$$

Where

$$A_{ij} = \sum_{k=1}^{N} \overline{(Q_{ij})_k}\,(h_k - h_{k-1})$$

$\overline{(Q_{ij})_k}$ are components of reduced stiffness matrix and $h_k - h_{k-1}$ is thickness of k^{th} layer.

Table 1 Quasi-static testing results for glass/carbon/epoxy hybrid laminates (4 Layers)

Sp. No	Thickness (mm)	Width (mm)	Area (mm^2)	Tensile stress (MPa)	Failure strain (%)	Tensile modulus (GPa)
2QG-1	1.89	6.0	11.34	380.2	8.21	7.77
2QG-2	1.96	6.1	11.97	383.4	7.46	8.17
2QG-3	1.68	5.9	09.92	424.5	6.5	9.82
Avg				**396.1 ± 24.7**	**7.40 ± 0.84**	**08.60 ± 1.08**
2QGC-1	1.920	6.0	11.52	442	6.00	12.46
2QGC-2	1.859	6.1	11.34	432.9	6.10	12.35
2QGC-3	2.02	6.0	12.16	387.6	5.85	11.83
Avg				**420.8 ± 29.1**	**5.98 ± 0.12**	**12.21 ± 0.33**
2QC-1	1.706	6.0	10.24	517.6	2.84	31.03
2QC-2	1.706	6.0	10.24	525.5	2.87	32.66
2QC-3	1.727	6.2	10.71	531.9	3.02	33.77
Avg				**525.0 ± 7.1**	**2.91 ± 0.09**	**32.49 ± 1.38**

Where, QG = quasi- static glass/epoxy composite, QGC = quasi-static glass-carbon/epoxy composite, QC = quasi- static carbon/epoxy composite

Table 2 High strain rate experimental results of glass/epoxy composites (4 layers)

Height (m)	Strain rate (s^{-1})	Tensile stress (MPa)	Tensile modulus (GPa)	Failure strain (%)
Quasi-static	0.001	396.1 ± 24.7	08.59 ± 1.08	7.40 ± 0.84
0.25	221.4	407.7 ± 17.0	27.63 ± 0.55	2.88 ± 0.25
0.5	313.2	434.0 ± 36.7	28.25 ± 0.35	2.55 ± 0.17
0.75	383.6	488.5 ± 40.0	30.81 ± 2.45	2.40 ± 0.18
1.0	442.9	517.4 ± 23.1	31.43 ± 5.64	2.19 ± 0.21
1.25	495.2	577.2 ± 51.1	31.58 ± 3.37	1.95 ± 0.05
1.5	542.4	658.8 ± 43.4	32.88 ± 0.55	1.82 ± 0.52

Table 3 High strain rate experimental results of hybrid (glass-carbon/epoxy) composites (4 layers)

Height (m)	**Strain rate (s^{-1})**	**Tensile stress (MPa)**	**Tensile modulus (GPa)**	**Failure strain (%)**
Quasi-static	0.001	420.8 ± 29.1	12.21 ± 0.33	5.98 ± 0.12
0.25	221.4	430.1 ± 5.6	29.31 ± 0.77	2.39 ± 0.65
0.5	313.2	440.1 ± 8.9	30.14 ± 1.55	2.06 ± 0.66
0.75	383.6	463.2 ± 31.0	32.03 ± 8.94	1.82 ± 0.27
1.0	442.9	475.2 ± 31.6	33.70 ± 4.22	1.57 ± 0.18
1.25	495.2	534.8 ± 30.0	34.21 ± 2.00	1.37 ± 0.35
1.5	542.4	585.3 ± 47.1	34.60 ± 7.63	1.30 ± 0.12

Table 4 High strain rate experimental results of carbon/epoxy composites (4 layers)

Height (m)	**Strain rate (s^{-1})**	**Tensile stress (MPa)**	**Tensile modulus (GPa)**	**Failure strain (%)**
Quasi-static	0.001	525.0 ± 7.1	32.49 ± 1.38	2.91 ± 0.09
0.25	221.4	556.3 ± 52.2	39.54 ± 1.29	1.81 ± 0.46
0.5	313.2	542.5 ± 43.2	40.34 ± 0.95	1.74 ± 1.03
0.75	383.6	529.8 ± 17.7	41.88 ± 6.58	1.72 ± 0.41
1.0	442.9	550.9 ± 50.6	43.51 ± 2.34	1.52 ± 0.26
1.25	495.2	550.5 ± 12.8	37.56 ± 5.96	1.28 ± 0.05
1.5	542.4	558.4 ± 16.6	42.46 ± 1.02	1.09 ± 0.01

5.2. Strain analysis

The DIC system is used to obtain the strain data. Specimen failure images are captured during loading condition by Phantom V611 high speed camera. The camera is set at a distance of 50 cm from the specimen with 128 X 128 resolutions with an exposure time of 9.81 µs and aparture of 2.8 cm. The LED lights are used to get good illustration. The VIC-2D software recognizes these images of DIC to obtain the in-plane displacements and strain contours. The accuracy of the measured displacements is influenced by the mean speckle size and the size of subset **[21]**. The subset size and step size are optimized to get reliable strain data. The colour map has chosen for DIC analysis as spectrum (cw). Typical strain contour

plots in the glass/epoxy, carbon/epoxy and hybrid (glass-carbon/epoxy) composites at 0.5 m height and at different time intervals are shown in Figs. 3-5.

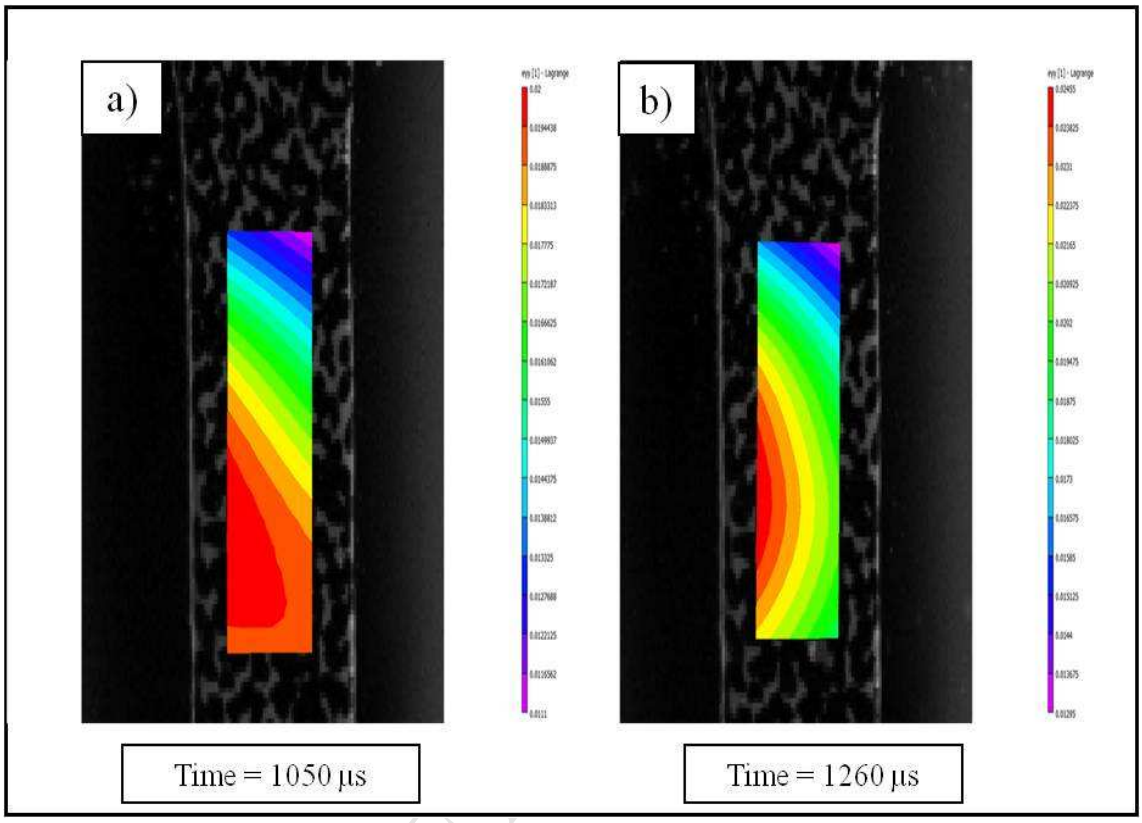

Fig. 3 Strain contour plots of the glass/epoxy composites at 0.5 m height a) $(\varepsilon_{yy})_{max} = 2\%$ at 1050 µs b) $(\varepsilon_{yy})_{max} = 2.4\%$ at 1260 µs

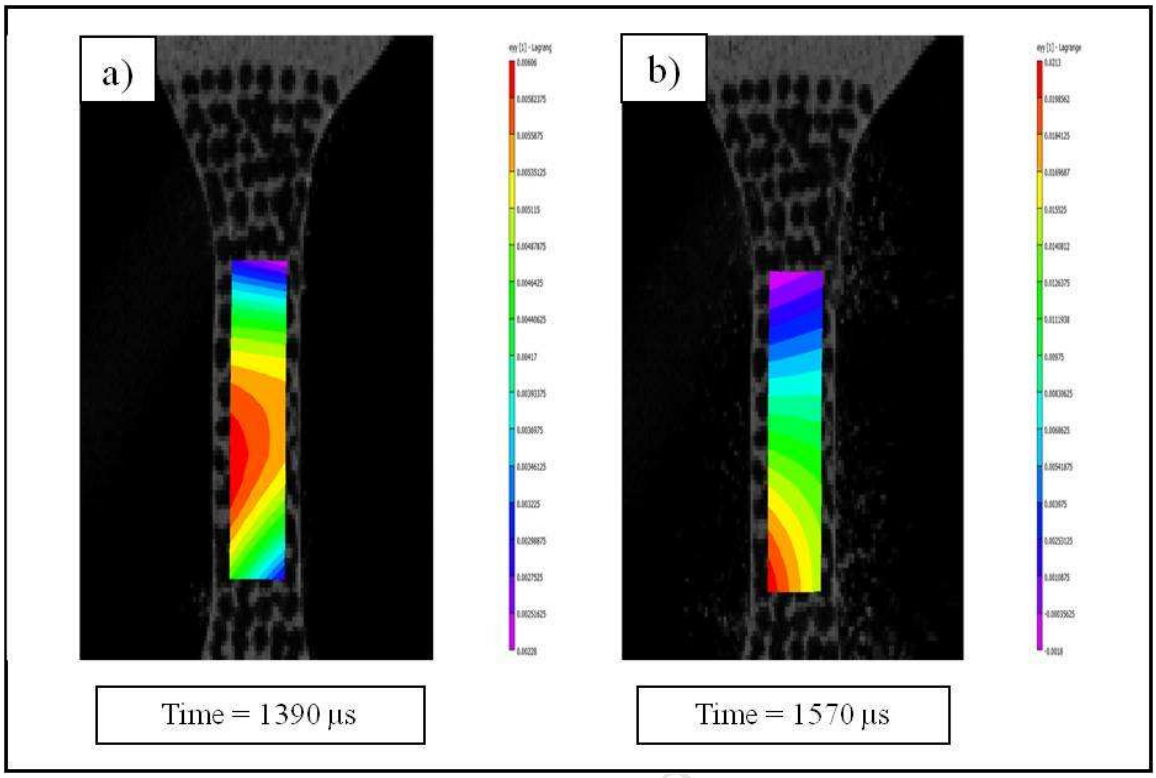

Fig. 4 Strain contour plots of the carbon/epoxy composites at 0.5 m height a) $(\varepsilon_{yy})_{max}$ = 0.6% at 1390 µs b) $(\varepsilon_{yy})_{max}$= 2% at 1570 µs

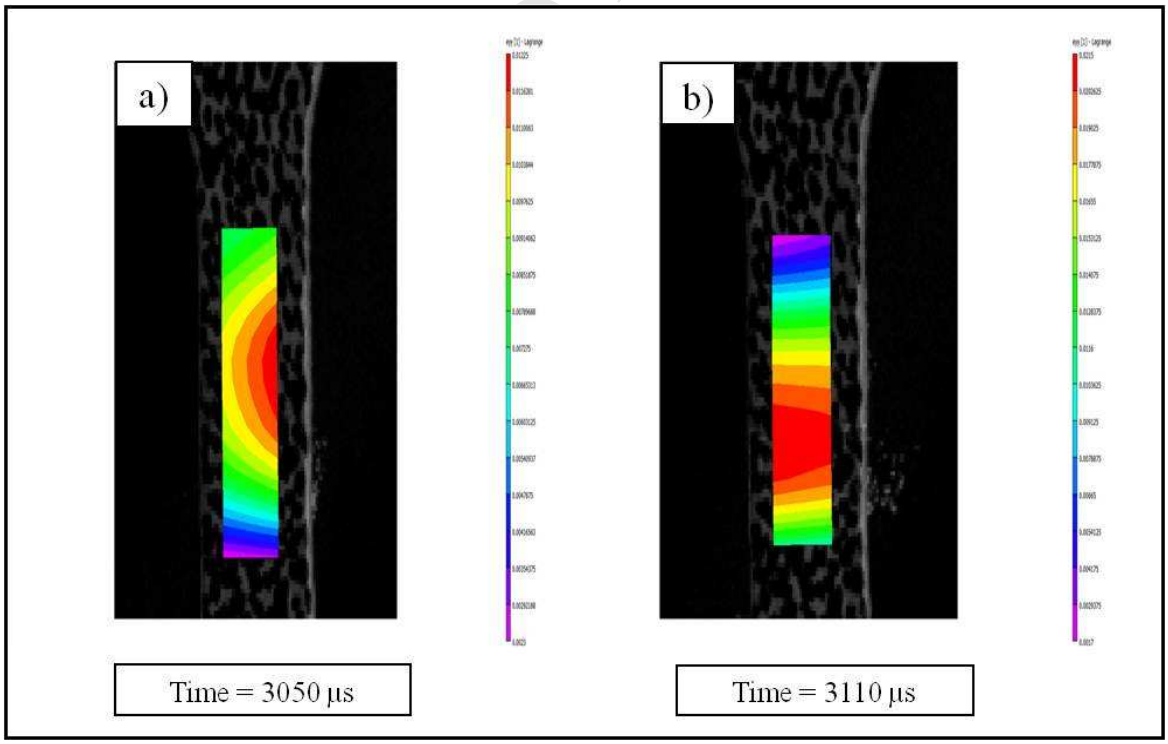

Fig. 5 Strain contour plots of the hybrid composites at 0.5 m height a) $(\varepsilon_{yy})_{max}$ = 1.2% at 3050 µs b) $(\varepsilon_{yy})_{max}$= 2.1% at 3110 µs

From Figs. 3 (b) ,4 (b) and 5 (b), it is seen that the failure strain obtained for glass/epoxy composites is 2.4%, for carbon/epoxy composites is 2% and hybrid (glass-carbon/epoxy) composites is 2.1 % at 1260 µs, 1570 µs and 3110 µs, respectively.

5.3 Effect of strain rate on mechanical properties

Yen and **Caiazzo (Y-C)** have used the logarithmic functions to measure strain rate effects in composites, **[22-25]** which are given by

$$y = E_{RT} = (E_0\, \varphi \ln \frac{\dot{\varepsilon}}{\dot{\varepsilon}_0} + E_0) \quad (4)$$

$$y = S_{RT} = (S_0\, \beta \ln \frac{\dot{\varepsilon}}{\dot{\varepsilon}_0} + S_0) \quad (5)$$

$$y = \varepsilon_{RT} = (\varepsilon_0\, \gamma \ln \frac{\dot{\varepsilon}}{\dot{\varepsilon}_0} + \varepsilon_0) \quad (6)$$

Where E_{RT} and E_0 are the rate adjusted (high strain rate) and quasi-static moduli, S_{RT} and S_0 are the rate adjusted (high strain rate) and quasi-static strengths, ε_{RT} and ε_0 are the high strain rate and quasi-static strains, respectively. $\dot{\varepsilon}_0$ is the reference strain rate = 1 s^{-1} and $\dot{\bar{\varepsilon}}$ are the effective strain rates. φ, β and γ are the strain rate constants for stiffness, strength and strain, respectively.

The first degree polynomial Eqn. is written as

$$y = mx + c \quad (7)$$

Where, m = slope of the line

By comparing Eqns. (4), (5), (6) with Eqn. (7)

y = E_{RT}, m = $E_0\, \varphi$, x = $\ln \frac{\dot{\varepsilon}}{\dot{\varepsilon}_0}$ in Eqn. (4); y = S_{RT}, m = $S_0\, \beta$, x = $\ln \frac{\dot{\varepsilon}}{\dot{\varepsilon}_0}$ in Eqn. (5); y = ε_{RT}, m = $\varepsilon_0 \gamma$, x = $\ln \frac{\dot{\varepsilon}}{\dot{\varepsilon}_0}$ in Eqn. (6);

Brown et al. [2] used the Y-C functions for their curve fitting and found that best curve fit is possible for strain rates above 36 s^{-1}. In the present research work, theoretical model is used based on strain rate dependent functions developed by Yen and Caiazzo **[22-25]** to determine the effect of strain rate on tensile modulus, tensile strength and tensile strain of the

composite specimens. Strain rate parameters for stiffness, strength and strain are determined by using the first degree polynomial equation (y = mx + c) and the known experimental values of the tensile modulus, tensile strength and failure strain. The obtained strain rate parameters (Table 5) are useful for numerical simulations and Engineering applications. Quasi-static experimental values are taken as reference values for theoretical model. The theoretical values of tensile modulus, tensile strength and tensile strain are determined from Eqns. (4), (5) and (6) by using the strain rate constants.

Table 5 Strain rate constants for glass/carbon/epoxy hybrid composites

Material type	**Strain rate constant for tensile modulus (φ)**	**Strain rate constant for tensile strength (β)**	**Strain rate constant for tensile strain (γ)**
Glass/epoxy	0.426	0.048	-0.116
Carbon/epoxy	0.046	0.006	-0.079
Hybrid	0.276	0.026	-0.118

It is observed from Table 1 that hybrid composites have higher tensile modulus compared to glass/epoxy composites and higher tensile failure strain than carbon/epoxy composites. From Table 2, it is observed that the tensile yield strength of glass/epoxy increases from 396.1 MPa at 0.0016 s^{-1} to 658.8 MPa at 542 s^{-1}, which indicates 66.3% increase in the tensile strength and the modulus has increased from 8.59 GPa to 32.8 GPa (3.8 times) for the same range of strain rates. It appears that as the strain rate increases, stiffening mechanism takes place, due to which there is an increase in modulus and strength. It is also observed for glass/epoxy composites that the failure strain decreases from 7.4% to 1.8% as the strain rate increases from 0.0016 s^{-1} to 542 s^{-1}. For hybrid (glass-carbon/epoxy) composites, the tensile strength and modulus have increased by 39% and 2.8 times, respectively for the same strain rate increase, whereas the failure strain decreases from 5.9% to 1.3% (Table 3). From Table 4, it is observed that the tensile yield strength of carbon/epoxy is insensitive to the strain rate. The modulus of carbon/epoxy increases from 32.4 GPa to 42.4 GPa (1.3 times) and failure strain of carbon/epoxy decreases from 2.9% to 1.09% as the strain rate increases. At quasi-static strain rates, the contact duration between the structure and loading device is more. Therefore, material tends to fail in ductile manner, whereas at higher strain rates, due to more loading rates, material tends to a more brittle behavior, which results into lower failure strain

at dynamic loading rates **[26-28]**. Theoretical results are validated with experimental results and are shown in Figs. 6 - 8. The results reveal that for GFRP, CFRP and hybrid composites, experimental values match well with the theoretical results.

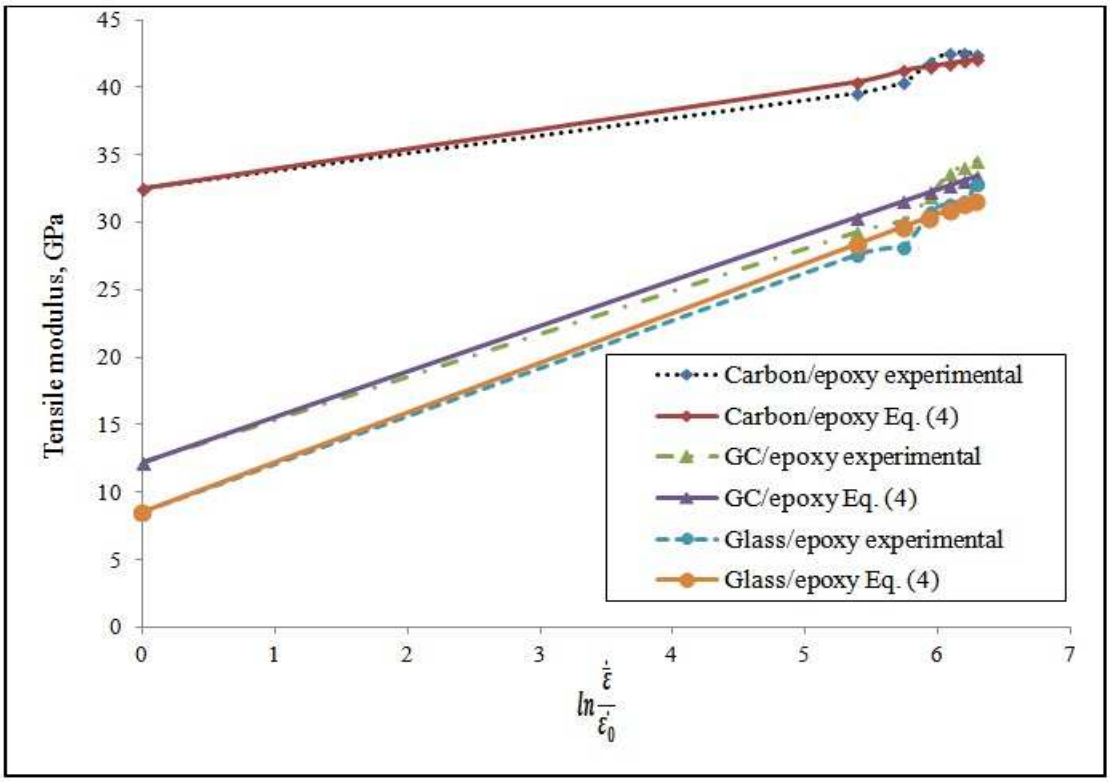

Fig. 6 The effect of strain rate on the tensile modulus of glass/carbon/hybrid composites

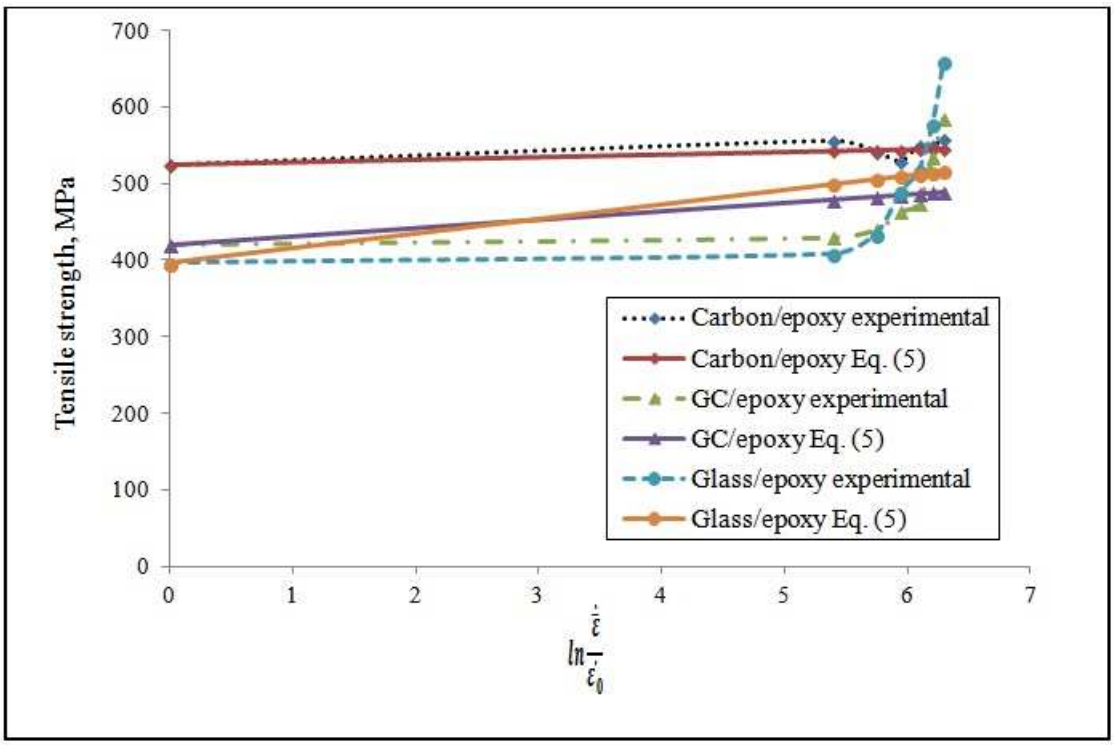

Fig. 7 The effect of strain rate on the tensile strength of glass/carbon/hybrid composites

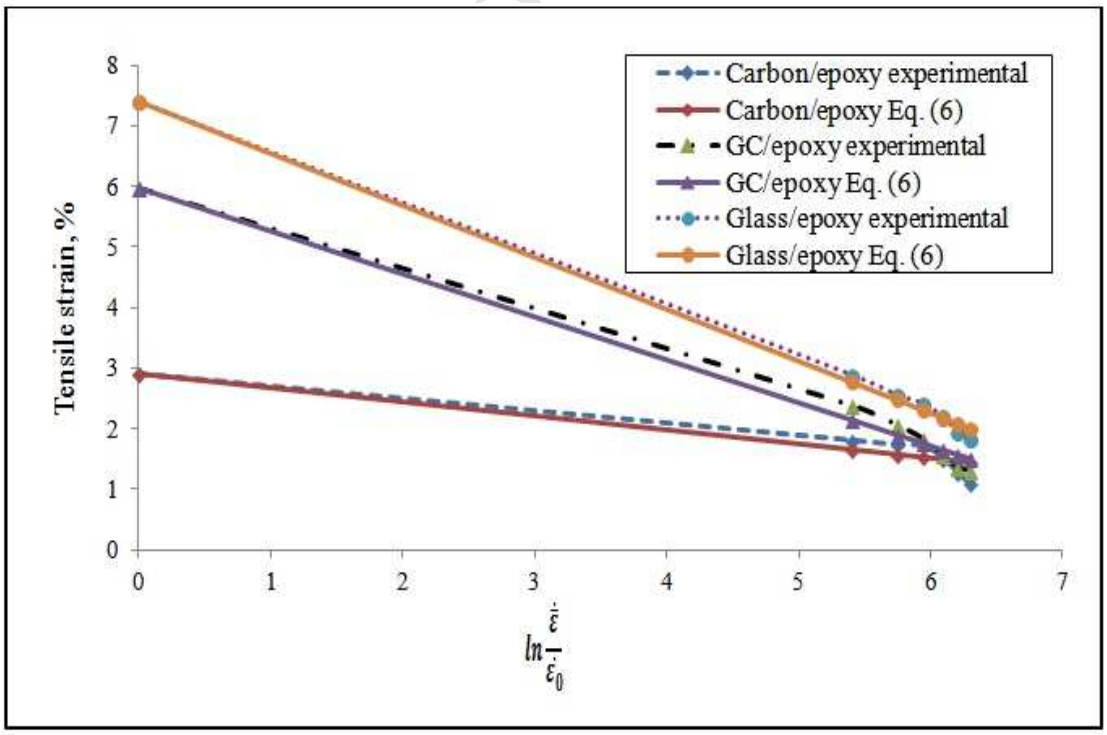

Fig. 8 The effect of strain rate on the tensile strain of glass/carbon/hybrid composites

The typical stress-strain response of the glass/carbon/hybrid/epoxy composites at different strain rates are shown in Figs. 9-11. Because of scattering in the response of the stress- strain curve, the polynomial regression of order 3 is chosen for plotting stress-strain curves. In quasi-static testing, it is observed that the stress-strain curve is linear elastic up to maximum stress. For dynamic loadings, due to nonhomogeneous deformation in the specimen and the viscoelastic behavior of matrix material followed by strain hardening cause the increase of tensile strength and modulus and decrease in failure strain. These variations are seen in Figs. 9-11. For glass/epoxy composites, even though both fiber and matrix are strain rate sensitive, the influence of strain rate sensitivity of matrix is less than the fibers **[29-30]**. Therefore, at dynamic loadings, tensile strength and modulus increase as strain rate increases, until the fibers fail completely.

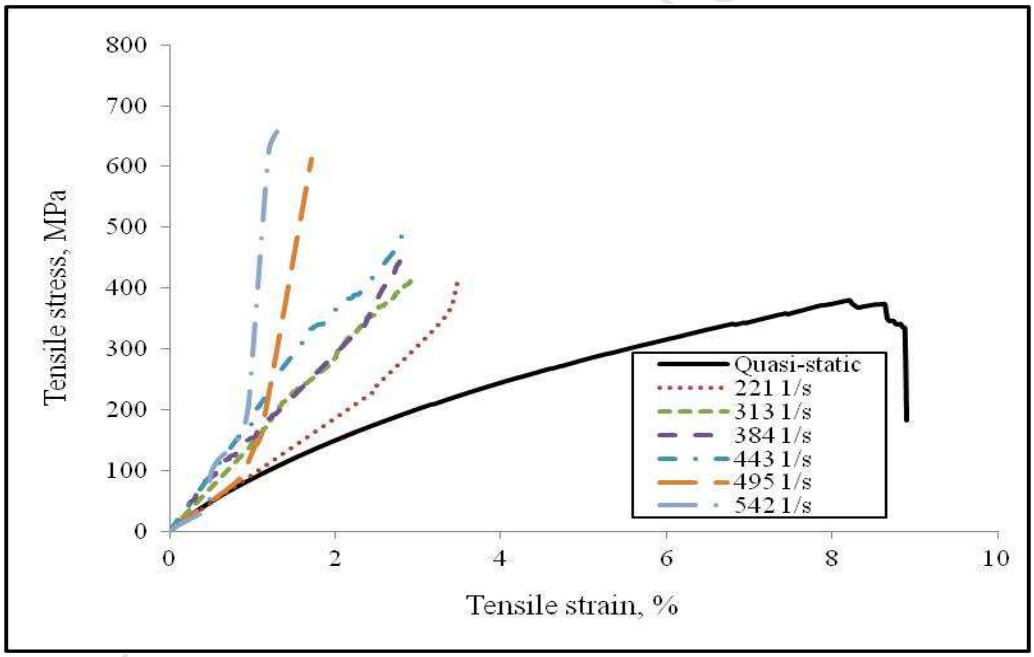

Fig. 9 Stress–strain response of GFRP composites for different high strain rates

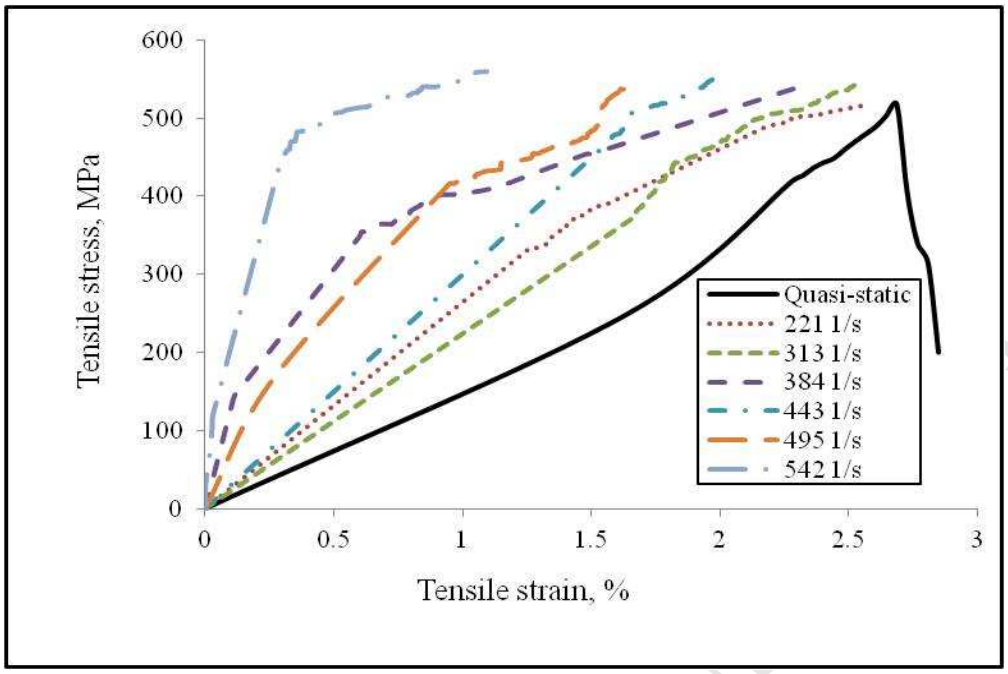

Fig. 10 Stress–strain response of CFRP composites for different high strain rates

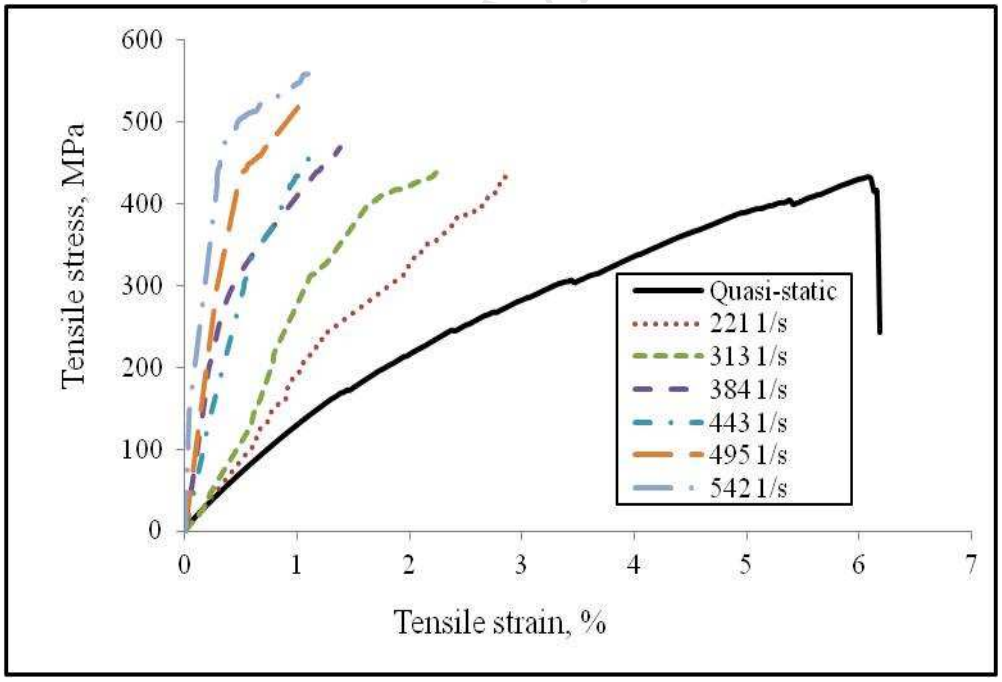

Fig. 11 Stress–strain response of hybrid composites for different high strain rates

6. Fractography analysis

SEM analysis was conducted on the tensile failed specimens for quasi-static and dynamic loadings by using Hitachi S-4800 Scanning Electron Microscope (SEM). The failed specimens were coated with an Ion-sputter coater equipment to obtain high conductance for SEM observation. The SEM micrographs of the glass/epoxy and carbon/epoxy composite specimens, tested under tensile loading are shown in Figs. 12 & 13.

It is observed in quasi-static tensile testing that the failure is progressive due to absence of inertia and wave propagation effects. Figs. 12 (a-c) indicate a failure mechanism (fiber breakage, fiber pull-out and matrix microcracking) in quasi-static tensile testing at a cross-head speed of 5 mm/min.

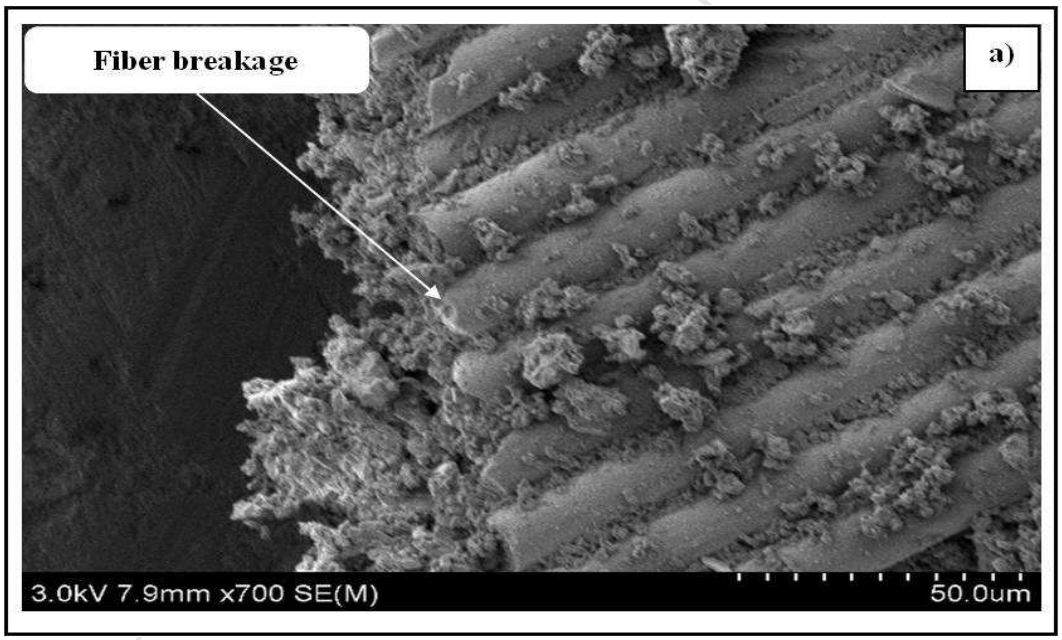

Matrix adhered to the fibers is shown in Figs. 12 (a), which indicate perfect bonding between fiber-matrix interface. Fiber - matrix adhesion induces brittle failure **[31]**. It is observed in Figs. 12 (a & b) that there is brittle failure and fiber breakage at the fiber ends.

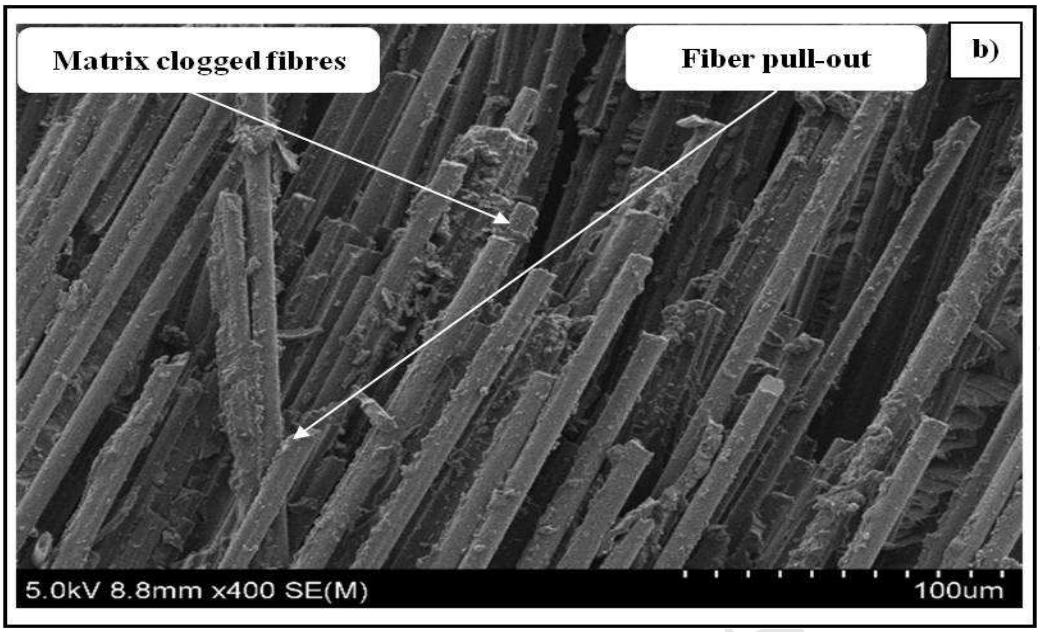

Fig. 12 (c) shows the river- line pattern along with microcracking in the resin of the cross ply laminates during quasi- static testing. This causes delamination in laminated composite plates, which lead to failure **[32-34].** Matrix microcracking also reduces the stiffness of the composite material **[35-36].**

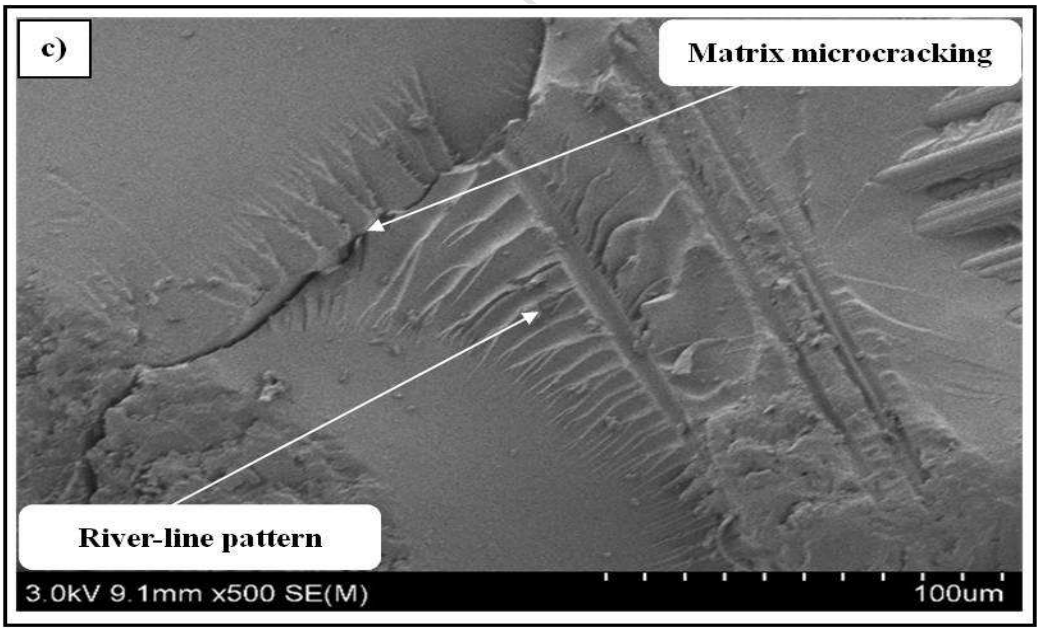

Fig. 12 SEM micrograph of the GFRP and CFRP composites in quasi-static tensile testing a) Fiber breakage (carbon/epoxy) b) Fiber pull-out (carbon/epoxy) c) Matrix microcracking (glass/epoxy)

The failure modes observed in high strain rate tensile testing show fiber pull-out , matrix crack, matrix damage and fiber – matrix interface debonding which are seen in Figs. 13 (a-c).

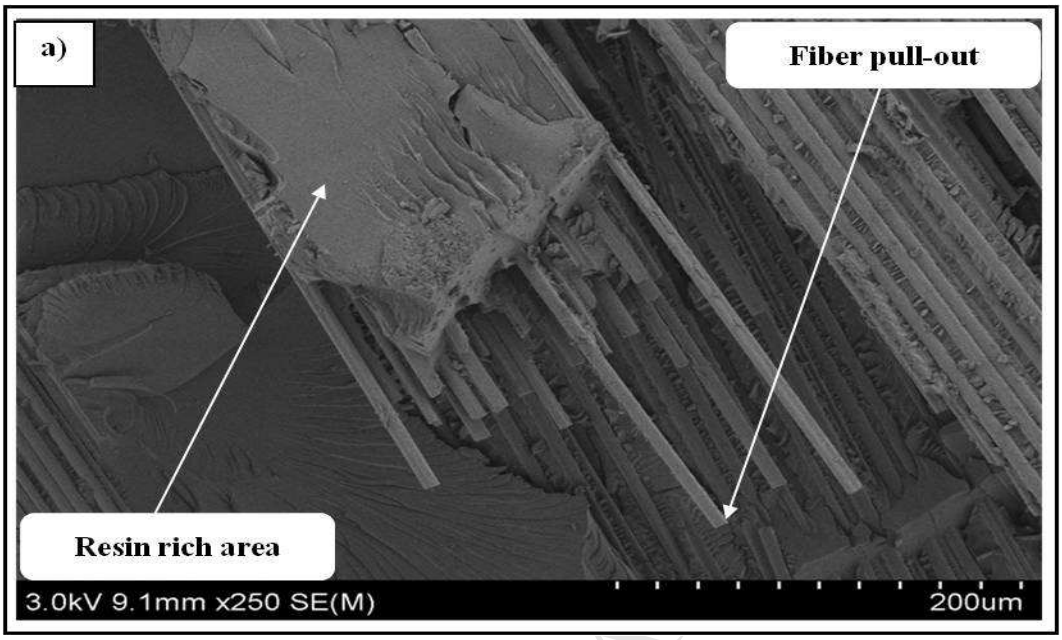

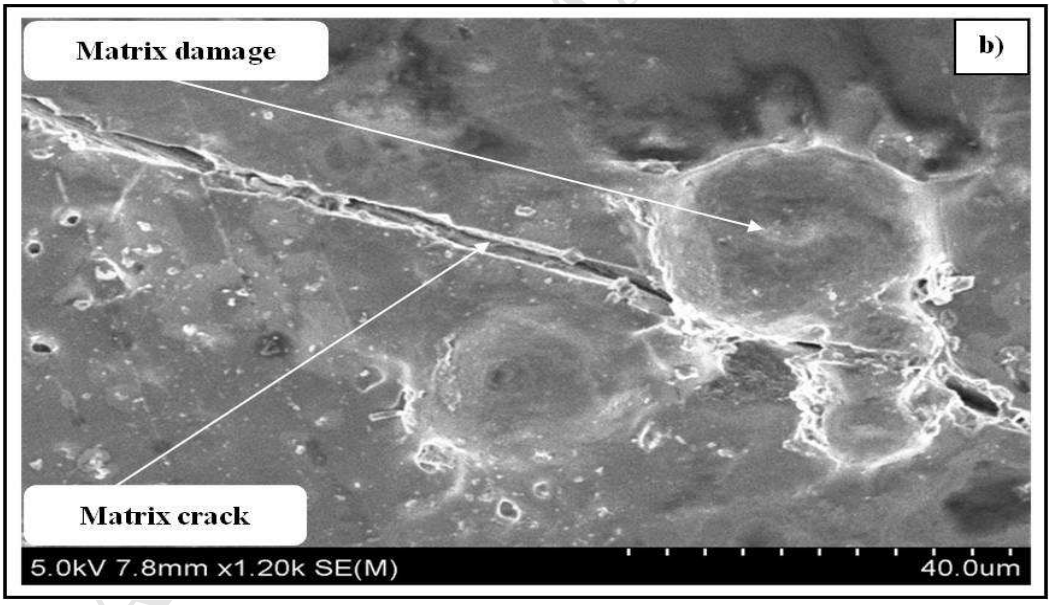

Matrix damage is dependent on the fiber-matrix interfacial bond strength and test speed. As strain rate increases, fibre tensile failure strength and tensile modulus have increased, which results in the increased fiber-matrix interfacial bond strength. The high strain rate loading causes matrix damage, which is seen in Fig. 13 (b). This leads the failure mechanism of fiber pull-out, which is seen in Figs. 13 (a). This occurs in the resin rich areas. Similar

observations are made in **[37].** It is observed that fiber – matrix debonding has occurred, which is seen in Fig. 13 (c).

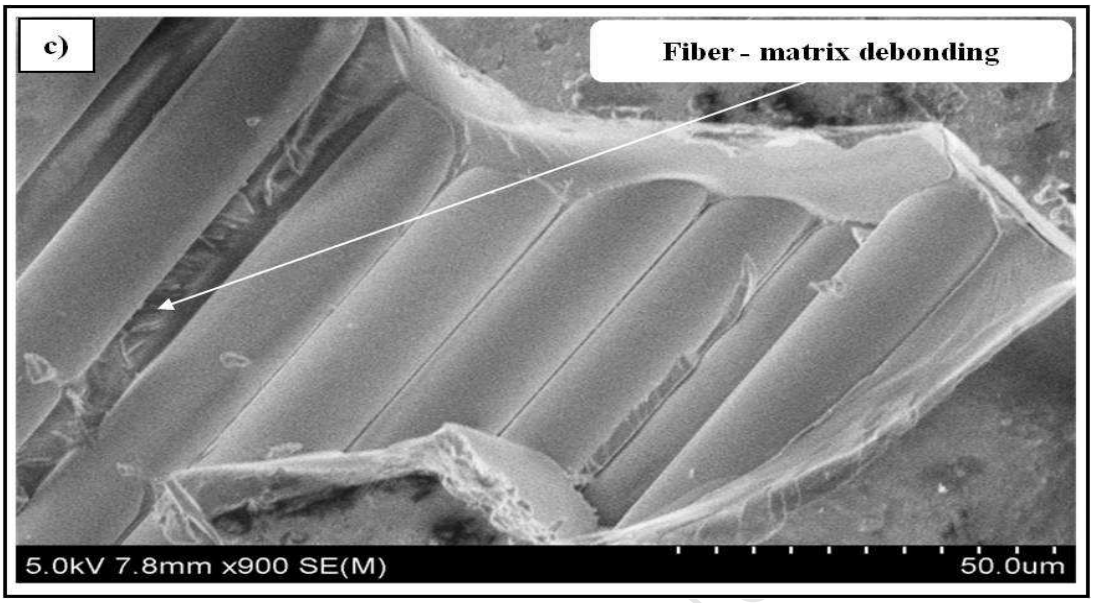

Fig. 13 SEM micrograph of the GFRP and CFRP composites at high strain rates a) Fiber pull-out (carbon/epoxy) b) Matrix damage and matrix crack (glass/epoxy) c) Fiber-matrix debonding (glass/epoxy)

7. Conclusions

In this work, an attempt is made to characterize the material behavior under tensile loading of glass/epoxy (GFRP), carbon/epoxy (CFRP) and hybrid (glass-carbon/epoxy) composites for strain rates ranging from 0.0016 s^{-1} to 542 s^{-1}. The following conclusions are drawn.

1. For glass/epoxy composites, the tensile strength (66.3%) and modulus (3.8 times) increased as the strain rate increases.
2. For carbon/epoxy composites, there is not much change in the tensile strength (6.3%) and modulus (1.3 times). Carbon/epoxy composites are stiffer materials and almost same load is required to break the specimens from quasi-static to dynamic loading rates. In general, both carbon fiber and epoxy matrix are brittle. The combination of these two materials exhibit almost same tensile strength and modulus from quasi-static to dynamic loading rates.

3. For hybrid (glass-carbon/epoxy) composites, the tensile strength and modulus increased by 39% & 2.8 times respectively, as the strain rate increases.
4. The failure strain in quasi-static testing is higher than that in dynamic loading for GFRP, CFRP and hybrid composites. At lower strain rates, due to less loading rates the failure takes place gradually. Whereas at higher strain rates, the conact duration between the structure and loading device is very less. Therefore, material tends to a more brittle behavior, which results into lower failure strain at high strain rates.
5. Glass/epoxy composites are the best combination out of three composites due to its more strain rate sensitivity. However, hybrid composites have combined advantageous of both glass/epoxy and carbon/epoxy composites. GFRP and CFRP composites have been made hybrid composites as sensitive to strain rate and also stiffer to impact loading.
6. The experimental results obtained in this study are useful to designers to validate numerical simulations with experimental values.
7. SEM micrographs of the tensile tested specimens show the rough surface, matrix crack, matrix damage, fiber pullout and fiber-matrix debonding during dynamic loading condition.
8. The best theoretical fit is obtained by the logarithmic functions for glass/carbon/hybrid composites. Experimental values match well with theoretical results.

Acknowledgment

The project is supported by ACECOST of ARDB, Structures Panel, India.

References

[1] Koerber H, Xavier J, Camanho PP. High strain rate characterization of unidirectional carbon-epoxy IM7-8552 in transverse compression and in-plane shear using digital image correlation. Mechanics of Materials 2010; 42: 1004–1019.

[2] Brown KA, Brooks R, Warrior NA. The static and high strain rate behavior of a commingled E-glass/polypropylene woven fabric composite. Composites Science and Technology 2010; 70: 272–283.

[3] Okoli OI. The effect of strain rate and failure modes on the failure energy of fiber reinforced composites. Composite structures 2001; 54: 299-303.

[4] Duan S, MO F, Yang X, Tao Y, Wu D, Peng Y. Experimental and numerical investigations of strain rate effects on mechanical properties of LGFRP composite. Composites Part B: Engineering 2016; 88: 101-107.

[5] Ochola RO, Marcus K, Nurick GN, Franz T. Mechanical behavior of glass and carbon fibre reinforced composites at varying strain rates. Composite Structures 2004; 63: 455–467.

[6] Gilat A, Goldberg RK, Roberts GD. Experimental study of strain-rate-dependent behavior of carbon/epoxy composite. Composites Science and Technology 2002; 62: 1469–1476.

[7] Elanchezhian C, VijayaRamnath B, Hemalatha J. Mechanical behavior of glass and carbon fibre reinforced composites at varying strain rates and temperatures. Procedia materials science 2014; 6: 1405 – 1418.

[8] Guedes RM, Vaz MA, Ferreira FJ and Morais JL. Response of CFRP Laminates under High Strain Rate Compression until Failure. Science and Engineering of Composite Materials 2005; 12: 145-151.

[9] Gurusideswar S and Velmurugan R. High strain rate sensitivity of glass/epoxy/clay nanocomposites. In: Proceedings of the 10th international conference on Composite Science and Technology, Lisbon, Portugal, 2015.

[10] Alemi-Ardakani M, Milani AS, and Yannacopoulos S. On complexities of impact simulation of Fiber Reinforced Polymer Composites: A simplified modeling framework. The Scientific World Journal 2014; Vol 2014.

[11] Rotem A and Lifshitz JM. Longitudinal strength of unidirectional fibrous composite under high rate of loading. In: Proceedings of the 26th Annual Technical Conference, Society of Plastics Industry, Reinforced Plastics/Composites Division, Washington, 1971.p.1–10.

[12] Gurusideswar S and Velmurugan R. Strain rate sensitivity of glass/epoxy composites with nanofillers. Materials and design 2014; 60: 468-478.

[13] Gurusideswar S, Velmurugan R and Gupta NK. High strain rate sensitivity of epoxy/clay nanocomposites using non-contact strain measurement. Polymer 2016; 86: 197-207.

[14] Naik NK, Ramasimha R, Arya H, Prabhu SV, ShamaRao N. Impact response and damage tolerance characteristics of glass – carbon hybrid composite plates. Composites Part B: Engineering 2001; 32: 565 – 574.

[15] Zweben C. Tensile strength of hybrid composites. Journal of Materials Science 1976; 12: 1325- 1337.

[16] Zweben C. In: Proceedings of the International Conference on Composite Materials, Geneva and Boston, 1975.

[17] Bunsell AR, Harris B. Hybrid carbon and glass fibre composites. Composites 1974; 5: 157-164.

[18] Groves SE, Sanchez RJ, Lyon RE and Brown AE. High strain rate effects for composite materials. Composite Materials: Testing and Design, ASTM STP 1206, ed. Camponeschi ET, American Society for Testing and Materials, Philadelphia, 1993; 11: 162-176.

[19] Hsiao HM and Daniel IM. Strain rate behavior of composite materials. Composites Part B: Engineering, 1998; 29 B: 521-533.

[20] Shirinbayan M, Fitoussi J, Meraghni F, Surowiec B, Bocquet M, Tcharkhtchi A. High strain rate visco-damageable behavior of Advanced Sheet Molding Compound (A-SMC) under tension. Composites Part B: Engineering 2015; 82: 30-41.

[21] Lecompte D, Smits A, Bossuyt S, Sol H, Vantomme J, Van Hemelrijck D, Habraken AM. Quality assessment of speckle patterns for digital image correlation. Optics and Lasers in Engineering 2006; 44: 1132-1145.

[22] Yen C-F. Ballistic impact modeling of composite materials. In: Proceedings of the 7th International LS-DYNA Users Conference. Dearborn, Michigan, 2002. p.15–26.

[23] Gillespie JJW, Gama BA, Cichanowski CE, Xiao JR. Interlaminar shear strength of plain weave S2-glass/SC79 composites subjected to out-of-plane high strain rate compressive loadings. Composites Science and Technology· 2005; 65(11-12): 1891-1908.

[24] Yen CF, Caiazzo A. Innovative processing of multifunctional composite armor for ground vehicles. ARL Technical Report ARL-CR-484, US Army Research Laboratory, Aberdeen Proving Ground, MD; 2000.

[25] Balkan O, Demirer H, SabriKayali E. Effects of deformation rates on mechanical properties of PP/SEBS blends. Journal of Achievements in Materials and Manufacturing Engineering 2011; 47.

[26] Roland CM, Twigg JN, Vu Y, Mott PH. High strain rate mechanical behavior of polyurea. Polymer 2007; 48: 574-578.

[27] Armenakas AE and Sciammarella CA. Response of glass-fiber-reinforced epoxy specimens to high rates of tensile loading. Experimental Mechanics 1973; 13: 433-440.

[28] Gilat A, Goldberg RK, Roberts GD. Strain Rate Sensitivity of Epoxy Resin in Tensile and Shear Loading, March 2005.

[29] Staab GH, Gilat A. High strain rate response of angle-ply glass/epoxy laminate. Journal of Composite Materials 1995; 29: 1308–1320.

[30] Staab GH, Gilat A. High strain rate characterization of angle-ply glass/epoxy laminates. In: Proceedings of the 9th international conference on composite materials, ICCM IX, Madrid, Spain, 1993.p.278–285.

[31] Yeung P, Broutman LJ. The effect of glass-resin interface strength on the impact strength of fiber reinforced plastics. Polymer Engineering and Science 1978; 18: 62-72.

[32] Liu S, Nairn JA. Fracture Mechanics Analysis of Composite Microcracking: Experimental Results in Fatigue. In: Proceedings of the 5th Technical Conference on Composite Materials, American Society of Composites, East Lansing, Michigan, 1990. p.11-14.

[33] Nairn JA, Hu S. The Initiation and Growth of Delaminations Induced by Matrix Microcracks in Laminated Composites. International Journal of Fracture 1992; 57: 1-24.

[34] Nairn JA. Matrix Microcracking in Composites. Polymer matrix composites 2000; 2: 403-432.

[35] Highsmith AL, Reifsnider KL. Stiffness-reduction mechanisms in composite laminates. Damage in Composite Materials, ASTM STP 1982; 775: 103-117.

[36] Fitoussi J, Bocquet M, Meraghni F. Effect of the matrix behavior on the damage of ethylene-propylene glass fiber reinforced composite subjected to high strain rate tension. Composites Part B: Engineering 2013; 45: 1181-1191.

[37] Okoli OI, Smith JF. Failure modes of fibre reinforced composites: The effects of strain rate and fibre content. Journal of Materials Science 1998; 33: 5415-5422.

Figure captions

Figure 1 Schematic diagram of drop tower a) Test setup model b) Specimen fixture c) Experimental setup

Figure 2 High strain rate specimen geometry a) AutoCAD diagram b) GFRP composites specimen c) Hybrid (glass-carbon/epoxy) composites specimen d) CFRP composites specimen

Figure 3 Strain contour plots of the glass/epoxy composites at 0.5 m height a) $(\varepsilon_{yy})_{max} = 2\%$ at 1050 µs b) $(\varepsilon_{yy})_{max} = 2.4\%$ at 1260 µs

Figure 4 Fig. 4 Strain contour plots of the carbon/epoxy composites at 0.5 m height a) $(\varepsilon_{yy})_{max} = 0.6\%$ at 1390 µs b) $(\varepsilon_{yy})_{max} = 2\%$ at 1570 µs

Figure 5 Fig. 5 Strain contour plots of the hybrid composites at 0.5 m height a) $(\varepsilon_{yy})_{max} = 1.2\%$ at 3050 µs b) $(\varepsilon_{yy})_{max} = 2.1\%$ at 3110 µs

Figure 6 The effect of strain rate on the tensile modulus of glass/carbon/hybrid composites

Figure 7 The effect of strain rate on the tensile strength of glass/carbon/hybrid composites

Figure 8 The effect of strain rate on the tensile strain of glass/carbon/hybrid composites

Table captions